HHS Public Access

Author manuscript

Nat Immunol. Author manuscript; available in PMC 2010 October 01.

Published in final edited form as:

Nat Immunol. 2010 April ; 11(4): 335–343. doi:10.1038/ni.1847.

A *Slfn2* mutation causes lymphoid and myeloid immunodeficiency due to loss of immune cell quiescence

Michael Berger[1], **Philippe Krebs**[1], **Karine Crozat**[1,2], **Xiaohong Li**[1], **Ben A. Croker**[1,3], **Owen M. Siggs**[1], **Daniel Popkin**[4], **Xin Du**[1], **Brian R. Lawson**[4], **Argyrios N. Theofilopoulos**[4], **Yu Xia**[1], **Kevin Khovananth**[1], **Eva Marie Y. Moresco**[1], **Takashi Satoh**[5], **Osamu Takeuchi**[5], **Shizuo Akira**[5], and **Bruce Beutler**[1]

[1]Department of Genetics, The Scripps Research Institute, 10550 North Torrey Pines Road, La Jolla, CA 92037, USA

[4]Department of Immunology and Microbial Sciences, The Scripps Research Institute, 10550 North Torrey Pines Road, La Jolla, CA 92037, USA

[5]Department of Host Defense, Research Institute for Microbial Diseases, Osaka University, 3-1 Yamada-oka, Suita, Osaka 565-0871, Japan

Abstract

We describe a new form of inherited immunodeficiency revealed by an *N*-ethyl-*N*-nitrosourea (ENU)-induced mutation called *elektra*. Homozygotes showed enhanced susceptibility to bacterial and viral infections, and diminished numbers of T cells and inflammatory monocytes that failed to proliferate upon infection and died via the intrinsic apoptotic pathway in response to diverse proliferative stimuli. *Elektra* mice exhibited an increased proportion of T cells poised to replicate DNA and their T cells expressed a subset of activation markers, suggestive of a semi-activated state. The *elektra* phenotype was positionally ascribed to a mutation in the gene encoding Schlafen-2 (*Slfn2*). Our findings reveal a physiological role for *Slfn2* in the defense against pathogens through regulation of quiescence in T cells and monocytes.

The immune system maintains a vast repertoire of B cells and T cells waiting to respond to microbial invasion. These quiescent, naïve lymphocytes may be activated by antigen engagement and costimulation, triggering an exit from the G0 phase of the cell cycle, entry into active cell cycle and increased metabolism as cells both expand and acquire effector functions. Previous studies demonstrate that lymphocyte quiescence, a state of reversible growth arrest in which cells remain responsive to activating stimuli and resistant to apoptosis (and are therefore not anergic), must be actively maintained by the action of

Correspondence should be addressed to B.B. (bruce@scripps.edu)..

[2]Current address: Centre d'Immunologie de Marseille-Luminy, Marseille, France

[3]Current address: Cancer and Haematology Division, The Walter and Eliza Hall Institute of Medical Research, 1G Royal Parade, Parkville, Victoria 3050, Australia

Author contributions M.B. and B.B. designed the research with critical suggestions from P.K., K.C., and A.N.T.; M.B., P.K., K.C., X.L., B.A.C., O.M.S., D.P., and B.R.L. performed experiments; X.L. and X.D. generated the BAC transgenic mice. M.B., Y.X. and K.K. performed all genome mapping. T.S., O.T., and S.A. generated *Slfn3*$^{-/-}$ and *Slfn1*$^{-/-}$ mice. M.B., E.M.Y.M., and B.B. wrote the manuscript.

molecules including transcription factors and cell cycle regulators1. DNA microarray experiments suggest that specific transcriptional programs are associated with the quiescent state2,3 and that cellular activation involves not only increased expression of genes that promote growth and differentiation, but also suppression of a quiescent gene expression program4,5. A growing number of known genes, including *Foxo1, Foxo2, Foxo3* (ref. 6), *Klf2* (ref. 7), and *Tob*8, have been implicated in the regulation of immune cell quiescence.

Here we describe an inherited immune deficiency characterized by susceptibility to both bacterial and viral infections, in which thymocytes develop normally, but peripheral T cells die in response to activating or homeostatic expansion stimuli. Activation also triggers death of inflammatory monocytes. The majority of peripheral T cells display a semi-activated phenotype, and this population of cells specifically undergoes apoptosis through the intrinsic apoptotic pathway. The mutational cause of this immune deficiency was positionally ascribed to the *Slfn2* gene, demonstrating for the first time a role for *Slfn2* in maintaining quiescence in immune cells *in vivo*.

Results

Immunodeficiency of *elektra* mutant mice

The recessive *elektra* phenotype was detected among G3 mice homozygous for random germline mutations induced by *N*-ethyl-*N*-nitrosourea **(**ENU). Mice were screened for mutations causing a lethal outcome following inoculation with normally sublethal quantities of mouse cytomegalovirus (MCMV)9. *Elektra* homozygotes died 6–8 days after inoculation with 2×10^5 PFU of MCMV, whereas nearly all C57BL/6J wild-type control mice survived (Fig. 1a). Serum cytokine concentrations in *elektra* homozygotes were comparable to those in wild-type mice for this infection model (Supplementary Fig. 1a), suggesting that this mutation did not confer an innate immune sensing defect. Moreover, the *elektra* mutation did not impair natural killer (NK) cell function, which is critical for controlling MCMV infection10, since killing of NK target cells and interferon-γ (IFN-γ) production upon activation of NK cells was intact (Supplementary Fig. 1b,c). The susceptibility phenotype was completely rescued by bone marrow transplantation from wild-type mice (Fig. 1b), suggesting that a hematopoietic defect was responsible for this phenotype. Further characterization demonstrated that the immune defect in *elektra* homozygotes was not restricted to the containment of MCMV infection. Lymphocytic choriomeningitis virus (LCMV; Armstrong strain) proliferated excessively in homozygous *elektra* mutants, while it was effectively cleared from wild-type mice by 7 days post-infection (Fig. 1c). Moreover, *elektra* homozygotes died 4–5 days after intravenous injection with *Listeria monocytogenes* due to impaired ability to control bacterial growth. The magnitude of susceptibility was similar to that observed in mice deficient in Toll-like receptor (TLR) signaling due to mutation in the *Myd88* gene, which encodes a critical TLR adapter protein (Fig. 1d and Supplementary Fig. 1d)11. Thus, despite normal innate sensing, homozygous *elektra* mice show susceptibility to diverse infections stemming from a defect in the hematopoietic compartment.

A defect in peripheral T cells

To characterize the immunological defect caused by the *elektra* mutation we performed immunophenotyping using flow cytometry. *Elektra* homozygotes showed normal cellularity of the spleen, thymus, lymph nodes, and peripheral blood. Low percentages of $CD4^+$ and $CD8^+$ T cells were evident both in the spleen and lymph nodes. The percentage of $CD8^+$ T cells was markedly reduced in blood, while the percentage of $CD4^+$ T cells was slightly reduced (Fig. 2a). However, thymic T cell populations were normal as assessed by double negative ($CD4^-$ $CD8^-$), double positive ($CD4^+CD8^+$) and single positive cell ratios, as well as total thymocyte numbers (Fig. 2b and data not shown). Control of LCMV infection is dependent upon $CD8^+$ T cell activity, and infection of wild-type mice with LCMV (Armstrong strain) leads to a sharp increase in $CD8^+$ T cell numbers. Consistent with their failure to restrict the proliferation of LCMV (Fig. 1c), *elektra* homozygotes showed a reduction in $CD8^+$ T cell numbers in response to LCMV infection (Fig. 2c, top). Moreover, restimulation of splenocytes from LCMV-infected *elektra* homozygotes *ex vivo* using LCMV-derived peptides (representing immunodominant epitopes of both envelope and nuclear protein antigens) revealed a severe reduction in the number of IFN-γ producing $CD8^+$ cells relative to wild-type (Fig. 2c, bottom). These findings demonstrate that the *elektra* mutation impaired both the number and the response of T cells

Activation signals lead to T cell death

To understand the peripheral T cell deficiency observed in *elektra* homozygotes, we first stimulated lymphocytes derived from lymph nodes with a combination of anti-CD3ε and anti-CD28, a combination of PMA and ionomycin, or with interleukin 2 (IL-2) for 72 h *in vitro*. Both $CD8^+$ and $CD4^+$ (data not shown) T cells from *elektra* homozygotes failed to expand normally in response to these stimuli (Fig. 3a). Further examination of the proliferative response to TCR activation using an *in vitro* bromo-2-deoxyuridine (BrdU) incorporation assay demonstrated that in fact a higher percentage of homozygous *elektra* $CD8^+$ T cells incorporated BrdU relative to wild-type after stimulation with anti-CD3ε plus CD28 for 24 h (Fig. 3b, left), indicating that *elektra* T cells are not growth arrested, and even contain an increased proportion of activation-competent cells. However, the opposite was observed after 48 h of activation, when fewer homozygous *elektra* $CD8^+$ T cells replicated DNA relative to wild-type (Fig. 3b, left). Consistent with these results, an elevated percentage of mutant $CD8^+$ T cells incorporated BrdU *in vivo* under steady state conditions (Fig. 3b, right). Annexin V staining 48 h after activation revealed massive apoptosis of mutant $CD8^+$ T cells (Fig. 3c). However, γ-irradiation-induced apoptosis was equivalent in homozygous *elektra* and wild-type $CD8^+$ T cells (Fig. 3d), indicating that the *elektra* mutation selectively causes death in response to activation.

Signals from the TCR control the activities of several pathways, including those of the transcription factors NF-κB and NFAT, and the Akt, Erk1/2, Jnk, and p38 mitogen-activated protein (MAP) kinase pathways, which together determine whether T cells will survive and proliferate or die through apoptosis12–16. We examined the activation status of each pathway within the first hour following TCR stimulation of wild-type or homozygous *elektra* $CD8^+$ T cells with anti-CD3ε- and anti-CD28-coated beads. We found normal TCR-stimulated calcium influx (Supplementary Fig. 2a), NFAT-dephosphorylation

(Supplementary Fig. 2b), NF-κB nuclear translocation (Supplementary Fig. 2c), and Erk and Akt phosphorylation in homozygous *elektra* cells (Supplementary Fig. 2d,e), demonstrating intact signaling through these T cell activation and survival pathways during the initial response to TCR stimulation. T cells from *elektra* homozygotes also exhibited normal induction of the activation markers CD25 and CD69 24 h after TCR activation (Supplementary Fig. 2f). However, p38-MAPK and Jnk, which are activated through phosphorylation, were constitutively phosphorylated under basal conditions, and further phosphorylated upon TCR stimulation in homozygous *elektra* $CD8^+$ T cells (Fig. 3e).

Collectively, these data demonstrate that compared to wild-type cells, homozygous *elektra* $CD8^+$ T cells initiate responses to TCR activation normally, with higher proportions of cells replicating DNA after 24 h of activation. By 48 h most *elektra* cells have become apoptotic. These results suggest that the *elektra* phenotype entails both hypersensitivity to an activating stimulus, as well as fragility following activation.

Elektra T cells die in response to expansion signals

To further test the proliferative capacity of homozygous *elektra* T cells, we examined their response to homeostatic proliferation signals. We adoptively transferred CFSE-labeled wild-type or homozygous *elektra* splenocytes (Ly5.2) into sublethally irradiated wild-type recipients (Ly5.1). Wild-type T cells underwent proliferation as expected, but no homozygous *elektra* T cells could be detected in the spleen 7 days after infusion (Supplementary Fig. 3a). When spleens were collected 2 and 4 days after adoptive transfer, a marked excess of the *elektra* homozygous mutant cells were found to be apoptotic as indicated by Annexin V staining (Fig. 4a). Homozygous *elektra* B cells were present in percentages similar to those of wild-type B cells in recipient mice (Supplementary Fig. 3b). To follow the fate of existing peripheral T cells, we blocked their replenishment with new thymic emigrants by thymectomy of adult mice. Wild-type T cell numbers declined by 30% following thymectomy and then remained stable for more than 60 days. In contrast, homozygous *elektra* T cells severely declined within 12 days after thymectomy and almost completely disappeared from the blood by 60 days after thymectomy (Fig. 4b).

We also tested homeostatic expansion of T cells in response to injection of IL-7 together with non-neutralizing anti-IL-7. This treatment mimics the lymphopenic condition and results in expansion of both T cells and B cells17. As expected, compared to injection with PBS, IL-7–anti-IL-7 injection resulted in expansion of both B and T cells, and a reduction in the percentage of Annexin V positive $CD8^+$ T cells after 6 days in wild-type mice (Fig. 4c). Whereas B cell populations expanded normally in *elektra* homozygotes, both $CD8^+$ and $CD4^+$ T cells failed to proliferate in response to IL-7–anti-IL-7 treatment (Fig. 4c). Moreover, in contrast to wild-type mice, a higher percentage of $CD8^+$ T cells from homozygous *elektra* mice were positive for Annexin V 6 days after IL-7–anti-IL-7 than after PBS injection (Fig. 4c, bottom), suggesting that they die in response to signals induced by IL-7.

The cell surface glycoprotein CD44 normally accumulates on T cells as they mature in the periphery: naïve T cells that have newly emigrated from the thymus express low amounts of CD44 while mature, expanding T cells express abundant CD44. *In vitro*, experimental

signals for homeostatic expansion also induce surface expression of CD44 (refs. 18–20). We examined Annexin V staining of $CD44^{hi}$ and $CD44^{lo}$ populations of splenic $CD8^+$ T cells from homozygous *elektra* and wild-type mice under steady state conditions. Regardless of genotype, most of the Annexin V positive cells were $CD44^{hi}$. While similar small percentages of wild-type and mutant $CD44^{lo}$ cells were Annexin V positive, the percentage of homozygous *elektra* Annexin V positive $CD44^{high}$ cells was significantly elevated over that of wild-type (Fig. 4d). Together, these findings demonstrate that homozygous *elektra* $CD44^{hi}$ $CD8^+$ T cells die in response to homeostatic expansion signals.

T cells die via the intrinsic apoptotic pathway

Homeostatic lymphoid cell death is required to eliminate cells that are no longer needed once an infection is resolved and to eliminate potentially autoreactive cells. It is mediated both by the intrinsic apoptotic signaling pathway (controlled by the balance of pro- and anti-apoptotic Bcl-2 family members), and the extrinsic apoptotic signaling pathway (controlled by signals from receptors for tumor necrosis factor (TNF), FasL, TRAIL). We examined the status of both pathways in homozygous *elektra* mice. We excluded the Fas-mediated extrinsic pathway as the mechanism of cell death in homozygous *elektra* T cells because no rescue of $CD8^+$ or $CD4^+$ T cells was observed in homozygous *elektra* $Fas^{lpr/lpr}$ double mutant mice (Fig. 5a).

The intrinsic pathway is chiefly responsible for T cell death after clonal expansion induced by acute, time-limited TCR activation that occurs during infection or homeostatic expansion21–23. The anti-apoptotic protein Bcl-2, which sequesters pro-apoptotic Bim and prevents activation of Bax and Bak, is a key regulator of apoptosis mediated by the intrinsic pathway24. Consistent with the finding that apoptosis of homozygous *elektra* T cells was increased in the $CD44^{hi}$ population (Fig. 4d), Bcl-2 expression was specifically reduced in the $CD44^{hi}$ population (Fig. 5b). Importantly, $CD4^+$ and $CD8^+$ T cell death was completely rescued in homozygous *elektra* mice expressing a *Bcl2* transgene (Fig. 5c). Moreover, the *Bcl2* transgene could partially restore the ability of homozygous *elektra* $CD4^+$ (data not shown) and $CD8^+$ T cells to proliferate *in vitro* in response to TCR stimulation (Fig. 5d). These results clearly demonstrate that death of homozygous *elektra* T cells is mediated by the intrinsic apoptotic pathway through the action of Bcl-2 family members and that T cells from *elektra* homozygotes have the capacity to proliferate once their propensity for apoptosis is blocked.

T cells exist in a semi-activated state

The $CD44^{hi}$ population encompasses both recently activated and memory phenotype cells, which may be discriminated on the basis of IL-2Rβ (CD122) expression, which is elevated in cells with a memory phenotype25. In wild-type spleen, the $CD44^{hi}$ $CD8^+$ T cell population was composed mostly of $CD122^+$ cells, but in homozygous *elektra* spleen, most of the $CD44^{hi}$ $CD8^+$ and $CD4^+$ T cells were $CD122^-$ (Fig. 6a, left, and Supplementary Fig. 4a, respectively). Induction of homeostatic T cell expansion in homozygous *elektra* mice by injection of IL-7–IL-7 antibody complex increased the percentage of cells with this altered CD122 expression (Fig. 6a, right). This $CD44^{hi}CD122^-$ population showed complete shedding of CD62L, absent expression of IL-7Rα (CD127) and low CD5 expression,

suggesting that these cells were recently activated (Fig. 6b, right). In addition, the $CD44^{lo}$ (naïve) population of $CD8^+$ and $CD4^+$ T cells in *elektra* homozygotes showed low expression of both IL-7Rα and CD62L (Fig. 6b, left, and Supplementary Fig. 4b). Low expression of CD62L, as opposed to complete shedding of the CD62L molecule, has been shown to occur in response to continuous TCR stimulation26,27. Similarly, low expression of IL-7Rα is associated with T cell activation. However, homozygous *elektra* $CD8^+$ T cells (both $CD44^{hi}$ and $CD44^{lo}$) express normal amounts of the CD69 activation marker (Fig. 6b) suggesting that they are not fully activated. $CD8^+$ T cells from *elektra* mice were also not exhausted, as indicated by normal expression of PD-1 (Fig. 6b). These findings strongly suggest that homozygous *elektra* T cells exist in a partially activated state that predisposes them to apoptosis in response to activation stimuli.

Surprisingly, although the *Bcl2* transgene rescued T cell death in *elektra* homozygotes (Fig. 5c), it did not prevent the development of a semi-activated phenotype by either $CD44^{hi}$ or $CD44^{lo}$ T cells from *elektra* homozygotes (Fig. 6c,d). Moreover, in non-lymphopenic mixed bone marrow chimeras [homozygous *elektra* (Ly5.2) and wild-type (Ly5.1) cells mixed 1:1 and transplanted into lethally irradiated *Cd3* deficient recipients], *elektra* T cells showed the same semi-activated phenotype (Fig. 6e,f). This result indicates that the semi-activated state, although exacerbated by lymphopenic conditions (Fig. 4a–c), is not primarily driven by the lymphopenic environment in homozygous *elektra* mice. Rather, it is intrinsic to *elektra* T cells and apoptosis is a consequence.

Monocytes die in response to activation signals

Inflammatory monocyte recruitment is essential for defense against *L. monocytogenes* in mice28. Since *elektra* homozygotes were highly susceptible to *L. monocytogenes*, we examined the inflammatory monocytes in these animals before and during infection. Prior to infection, *elektra* homozygotes showed a normal percentage of inflammatory monocytes in the bone marrow but slightly reduced percentages of these cells in the blood and spleen compared with wild-type mice (Fig. 7a, gated R1 population). Following infection, the fraction of inflammatory monocytes increased far less in the blood and spleen of *elektra* homozygotes relative to the increase observed in wild-type mice (Fig. 7a). No accumulation of inflammatory monocytes was observed in the bone marrow (Fig. 7a), indicating that a migration problem did not cause this aspect of the *elektra* phenotype. In contrast to inflammatory monocytes, a normal percentage of neutrophils was found in *elektra* homozygotes under steady state conditions. An increased percentage of neutrophils was found in *elektra* homozygotes following listeria infection, (Fig. 7a, gated R2 population). The exaggerated accumulation of neutrophils after infection may be attributed to the elevated bacterial burden in *elektra* homozygotes, as previously shown for CCR2-deficient mice28. Macrophage numbers and recruitment to the peritoneal cavity were normal in *elektra* homozygotes, as were macrophage responses to TLR ligands *in vitro* (data not shown). Dendritic cells (DCs) were present in normal numbers (data not shown), and when stimulated with unmethylated CpG oligonucleotides, these cells survived and upregulated the costimulatory molecule CD40 as effectively as wild-type cells (Supplementary Fig. 5). In mixed bone marrow chimeras [homozygous *elektra* (Ly5.2) and wild-type (Ly5.1) cells mixed 1:1 and transplanted into lethally irradiated *Cd3* deficient recipients], both T cells and

inflammatory monocytes derived from *elektra* homozygotes were markedly disfavored compared to cells of wild-type origin, while equal percentages of B cells and neutrophils of homozygous *elektra* and wild-type origin were observed (Fig. 7b). Together, these findings indicate a cell-intrinsic, lineage-specific effect of the *elektra* mutation.

We determined whether the $CD11b^{+}Ly6C^{hi}$ monocytes from homozygous *elektra* mice were more prone to apoptosis in response to bacterial stimuli. We sorted $CD11b^{+}Ly6C^{hi}$ $Ly6G^{-}$ monocytes from the bone marrow of uninfected mice, cultured the cells for 3 days *in vitro* in the presence of IFN-γ and heat-killed *L. monocytogenes*, and then examined the cells for activation and apoptosis markers by flow cytometry. After treatment, wild-type monocytes displayed an increase in major histocompatibility complex (MHC) class II expression (Fig. 7c, top) and nitric oxide (NO) secretion (Fig. 7c, bottom), and in their forward scatter/side scatter (FSC/SSC) profile, indicating that they became activated and differentiated (Fig. 7d). The percentage of wild-type Annexin V positive cells also decreased after treatment (Fig. 7e). In contrast, the majority of homozygous *elektra* monocytes failed to upregulate MHC class II (Fig. 7c, top), and NO could not be detected in the culture medium (Fig. 7c, bottom). The percentage of Annexin V positive *elektra* monocytes increased, and indeed most appeared to be dead, as indicated by their low FSC/SSC profile (Fig. 7d,e). These results demonstrate that similar to homozygous *elektra* T cells, monocytes also undergo apoptosis in response to activation.

A mutation in *Slfn2* causes the *elektra* phenotype

The mutation responsible for the *elektra* phenotype was mapped to Chromosome 11 by scoring for $CD8^{+}$ T cell deficiency in the blood (Supplementary Fig. 6a,b), and then further confined to a critical region 5.5 megabase (Mb) pairs in size bounded by the markers D11Mit34 and D11Mit119 (located 79 Mb and 83.5 Mb from the centromere, respectively) (Supplementary Fig. 6c). The critical region contained a total of 116 annotated candidate genes (Supplementary Fig. 6d). All coding exons in the region were targeted for automated sequencing, and 69.7% high quality coverage of mutant and control templates was achieved on first pass. A single point mutation was identified in the region within *Slfn2* (Supplementary Fig. 6e), which encodes one member of a paralogous family of proteins with largely unknown function. The mutation results in an isoleucine to asparagine substitution of residue 135 of the encoded 278 amino acid protein (Supplementary Fig. 6f). BAC transgenesis was used to rescue the *elektra* $CD8^{+}$ T cell phenotype, confirming the causative relationship between the mutation and the observed phenotype (Fig. 8a,b). We infer that *elektra* is a loss-of-function rather than a gain-of-function allele, first because the phenotype is recessive, and second because transgenesis with the wild-type sequence rescued the phenotype instead of worsening it. The listeria susceptibility and MCMV susceptibility were also abolished by transgene rescue (Fig. 8c,d).

In addition to study of $Slfn2^{elektra/elektra}$ mice, we generated $Slfn1^{-/-}$ and $Slfn3^{-/-}$ mice by gene targeting and examined their phenotypes. Consistent with a previous report29 $Slfn1^{-/-}$ mice showed no reductions in the numbers or frequencies of T cells, NK cells, monocytes or CD19-positive B cells in blood, spleen, lymph nodes, or thymus (Supplementary Fig. 7a). $Slfn3^{-/-}$ mice also displayed no evident immune phenotype (Supplementary Fig. 7b). We

conclude that Slfn2 has a non-redundant function in the regulation of peripheral T cell and inflammatory monocyte survival, while Slfn1 and Slfn3 do not.

Discussion

Our results demonstrate that a mutation in *Slfn2* causes immunodeficiency as a consequence of T cell and monocyte apoptosis secondary to a semi-activated phenotype. Multiple findings strongly suggest that this semi-activated state in *Slfn2*$^{elektra/elektra}$ T cells stems from a loss of cellular quiescence. First, homozygous *elektra* T cells display an elevated percentage of cells replicating DNA both in the steady state and during the initial response to TCR stimulation, suggestive of an increased readiness to enter S phase. Second, unstimulated homozygous *elektra* T cells display a unique phenotype in which naïve (CD44^{lo}) T cells express low amounts of CD62L and IL-7Rα, and mature (CD44^{hi}) T cells express no CD62L, IL-7Rα, or CD5, but normal expression of CD69, indicative of a semi-activated phenotype.

The activation of several pathways, including the NF-κB, NFAT, Akt, Erk1/2, Jnk, and p38 MAP kinase pathways, regulates T cell survival. In the case of homozygous *elektra* mutants, we presume that as a result of a loss of quiescence, the balance between these pathways is altered to favor apoptosis rather than expansion. Indeed, we observe that p38 MAPK and Jnk were constitutively activated in unstimulated *elektra* T cells. Activation of these kinases is associated with T cell apoptosis15,16, and may represent a factor contributing to apoptosis of *elektra* T cells. The enhancement of p38-MAPK and Jnk phosphorylation observed upon TCR stimulation of *elektra* T cells and the fact that inflammatory monocytes (of the myeloid lineage) also undergo apoptosis upon activation, together suggest that the proliferative signals negatively regulated by Slfn2 may be distinct from the TCR signaling pathways that lead to the development of activated T cell effector functions and full T cell activation.

Several studies suggest that lymphocytes must actively maintain a quiescent state in order to remain resistant to apoptosis. IL-15 has been shown to exert quiescence-inducing effects which are important for its anti-apoptotic properties30. Transcription factors that include members of the Foxo family6 and LKLF7,31 have also been shown to promote quiescence and loss of their activity leads to induction of apoptosis. However, several recent studies have challenged the idea that Foxo and LKLF regulate the quiescent state *per se*, presenting evidence that these proteins instead control expression of homing and survival proteins32–34. These reports suggest that impaired trafficking and survival of T cells create a lymphopenic environment that leads to the loss of quiescence in peripheral T cells, and raise the question of whether Slfn2 actually controls survival or quiescence of T cells. Death of homozygous *elektra* T cells was rescued by transgenic expression of the anti-apoptotic *Bcl2* gene. However, although T cells in these mice were not subject to a lymphopenic environment, they still showed the same semi-activated phenotype as T cells from homozygous *elektra* mice. Similarly, in mixed bone marrow chimeras, *elektra* T cells underwent apotosis and displayed a semi-activated phenotype, despite being in a normal, non-lymphopenic environment. Thus, our results indicate that the failure of mature homozygous *elektra* T cells to engage the anti-apoptotic machinery of the cell stems from loss of quiescence and acquisition of a semi-activated phenotype by naïve *elektra* T cells,

and is not a consequence of impaired survival signaling or activation by a lymphopenic environment. IL-7 and IL-15 are critical T cell growth and survival factors, and the absence of their signaling due to loss of IL-7Rα and IL-2Rβ expression in $CD44^{hi}$ T cells may be the trigger that activates the intrinsic apoptotic pathway in homozygous *elektra* T cells.

Slfn2 is one of 9 members of the *Slfn* gene family located in a cluster on mouse Chromosome 11 (ref. 29,35). A tenth Schlafen (Slfn) family member, Schlafen like 1 (*Slfnl1*), is encoded by a gene on Chromosome 4 (ref. 36). While *Slfn2* has no human orthologue, it is most similar to *SLFN12* and *SLFN12L*, two of seven paralogues encoded by the human genome. Aside from a divergent AAA domain (ATP binding Associated with cellular Activities) and a sequence designated COG2685 (NCBI Conserved Domain Database) found in all Slfns, Slfn2 bears no similarity to other proteins29,35. AAA (ATPases associated with various cellular activities) domains, to which the divergent AAA domain is related, are present in proteins of the AAA+ family, and mediate conformational and translocational changes of substrate proteins during cycles of nucleotide binding and hydrolysis37,38. COG2685, a domain of unknown function, is predicted to contain a helix-turn-helix DNA binding motif, and bears similarity to a domain present in several ATP-dependent DNA helicases and transcriptional regulators35. The *elektra* mutation, a T>A transversion, causes an isoleucine to asparagine substitution of residue 135 of the 278 amino acid Slfn2 protein, within a region in which no functional domains have been identified.

We hypothesize that Slfn2 maintains the quiescent state by promoting the expression of quiescence genes and/or repression of genes required for proliferation or differentiation. Previous work, primarily on the related Slfn1 protein (53% identical), supports this hypothesis. Thymocyte-specific transgenic expression of *Slfn1* cDNA in mice resulted in severe reduction of overall thymus size due to impaired development of the $CD4^{-}CD8^{-}$ double negative population in the thymus29. *In vitro*, ectopic expression of Slfn1 in fibroblasts represses cell growth and arrests cells in the G1 phase by causing transcriptional downregulation of cyclin D1 (refs. 29,35,39). Notably, relative to Slfn1, Slfn2 overexpression caused much stronger growth repression9. The *Cyclin D* genes are targets of Foxo transcription factors important in the regulation of quiescence6, raising the possibility that function of Slfn2 intersects with the pathways controlling Foxo function.

We have shown that the *elektra* allele of *Slfn2* confers susceptibility to two very different viral infections (LCMV and MCMV) in mice. Susceptibility to LCMV is likely related to impairment of $CD8^{+}$ T cell function. Interestingly, the mutation has no effect on NK cell numbers or function, although these cells are known to be essential for defense against MCMV. We consider it possible that inflammatory monocytes fulfill an essential function as well, given that lymphocytes are not needed for survival during the first several weeks following inoculation with MCMV10. Indeed, monocyte and macrophage cells are suggested to be protective in influenza infections40, and inflammatory monocytes are essential for defense against *L. monocytogenes* infection28. Recently, a non-redundant role was directly demonstrated for inflammatory monocytes in controlling viral infection41.

Several orthopoxviruses contain either full-length or fragmentary *Slfn* homologues. The full-length camelpox v-SLFN is most similar to mouse Slfn1 and Slfn2, with approximately 30%

amino acid identity in the conserved region. A recombinant vaccinia virus strain expressing camelpox v-SLFN is attenuated relative to the wild-type virus when mice are infected intranasally, resulting in reduced weight loss and more rapid recovery42. Viruses thus appear to have appropriated a *Slfn* sequence, and may use it to manipulate the survival and proliferation of host immune cells, and hence, the immunopathologic consequences of infection.

Methods

Mice and MCMV susceptibility screen

C57BL/6J (also referred to as WT), C3H/HeN, C57BL/6-*Cd3e*^{m1Btlr} and C57BL/6-*Myd88*^{poc} mice were maintained under specific pathogen-free conditions in The Scripps Research Institute vivarium, and all studies involving mice were performed in accordance with institutional regulations governing animal care and use. C57BL/6J mice, which are naturally resistant to MCMV, were used for mutagenesis as previously described43. The conditions of the *in vivo* MCMV susceptibility screen were described previously9. C57BL/6-*Tg(BCL2)25Wehi/J*, B6.MRL-*Faslpr/J* and C57BL/6.SJL (*Ptprc*^{a}*Pep3*^{b}*; Ly5.1*$^{+}$) were purchased from The Jackson Laboratory. The *elektra* strain may be obtained from the MMRRC, and is described at http://mutagenetix.scripps.edu.

MCMV, LCMV and *L. monocytogenes* infections

Preparation of the MCMV stock (Smith strain) was described previously9. Mice were infected with MCMV by intraperitoneal injection. The Armstrong strain of LCMV (provided by M.B.A. Oldstone, TSRI, La Jolla, CA) was injected intravenously. Viral loads were determined after organ homogenization in DMEM, 3% FCS by standard plaque assays on NIH-3T3 cells for MCMV and on VERO cells for LCMV. For *in vivo* challenge with *L. monocytogenes* (strain 10403S; Xenogen, Inc.), bioluminescent bacteria were prepared and injected intravenously as described previously44.

Genetic Mapping

Because most inbred strains show either a strong or moderate susceptibility to MCMV infection, the chromosome location of the *elektra* mutation was mapped using the low CD8 T cell phenotype. Initial confinement of the mutation was made by outcrossing *elektra* homozygotes to C3H/HeN mice, and then backcrossing F1 hybrids to the homozygous *elektra* stock. The percentage of CD8^{+} T cells in the blood of 6 week old F2 mice was analyzed by flow cytometry. Linkage was measured with respect to a panel of 129 markers distributed across the genome at 50 Mb intervals. Additional microsatellite markers were used in fine mapping studies.

Transgenesis

The BAC clone RP23-246H3, which represents a 197 Kb genomic DNA fragment between 82798126 and 82995557bp on Chr. 11, was obtained from CHORI (Children's Hospital Oakland Research Institute) and microinjected into the male pronucleus of >100 fertilized *Slfn2*$^{elektra/elektra}$ oocytes to produce transgenic animals. Embryos were transferred to pseudopregnant CD1 females and a total of 12 pups were born. Among them, 7 mice were

confirmed as transgenic founders by sequencing DNA amplified across the *Slfn2*^{elektra} mutation site. In the 5 remaining mice, only the mutant *Slfn2* sequence was present.

In vivo assay for NK cell cytotoxicity

In vivo assay for NK cell cytotoxicity preformed as previously described45.

Isolation of NK cells, CD8$^+$ T cells and monocytes

NK cells, CD8$^+$ T cells or DCs were isolated from spleens using the DX5 (CD49b) antibody (130-052-501), CD8$^+$ T cell isolation kit (130-090-859), or CD11c MACS cell separation kit (130-052-001), respectively, from Miltenyi Biotech according to the manufacturer instructions. For monocyte purification, bone marrow cells were stained with CD11b-APC (M1/70, eBioscience), Ly6C-Fitc (AL-21, BD Biosciences) and Ly6G-PE (1A8, Biolegend) antibodies. Then the CD11b$^+$, Ly6C^{hi} and Ly6G$^-$ sub population were sorted using FACS Aria (BD).

Ex vivo restimulation of CD8 cells

Splenocytes from LCMV-infected mice were restimulated with the indicated concentrations of LCMV peptides GP33 or NP396 for 4 h in the presence of brefeldin A (BD Biosciences), after which IFN-γ production was measured by intracellular staining.

In vitro T cell proliferation assay and BrdU incorporation assay

Lymph node or spleen cells were labeled with CFSE for 10 min followed by two wash steps. Cells were plated in 24-well plates that were coated with anti-CD3ε (10 μg/ml; eBioscience) and anti-CD28 (10 μg/ml; eBioscience), or plated in uncoated 24-well plates and then treated with mIL-2 (100 ng/ml; eBioscience) or PMA-ionomycin. Cells were collected at different time points and CFSE intensity was analyzed by flow cytometry.

For BrdU incorporation; after activation BrdU (BD Biosciences) was added for 90 min. Cells were stained with anti-BrdU antibody (3D4; BD Biosciences), followed by flow cytometric analysis

Adoptive transfer of T cells, thymectomy and bone marrow transplantation

For adoptive transfer, CFSE labeled spleen cells were injected intravenously into recipient mice that had been sublethally irradiated (600 rad) 24 h earlier. Seven days following adoptive transfer, splenocytes were prepared, surface stained for CD45.1 (A20, eBioscience) together with CD8 (53-6.7, eBioscience) or CD4 (L3T4, eBioscience) and then analyzed by flow cytometry for CFSE dilution.

Thymectomy was performed on 7 week old male mice by suction under ketamine (100 mg/kg) and Xylazine (10 mg/kg) anesthesia46. Mice with an incomplete thymectomy were excluded from analysis.

For bone marrow transplantation, bone marrow cells were extracted from femurs and tibias and were placed in PBS, 0.1% BSA (vol/vol). Bone marrow cells (5×10^6) were injected intravenously into the lateral tail veins of recipient mice that had been irradiated (1000 rad)

24 h earlier. For mixed bone marrow chimeras, equal numbers of bone marrow cells from congenic WT (C57BL/6.SJL) ($Ptprc^{a}Pep3^{b}$; $Ly5.1^{+}$) and homozygous *elektra* mice ($Ly5.2^{+}$) were injected into irradiated (1000 rad) CD3-deficient mice.

IL-7/anti-IL-7 mAb injection *in vivo*

1.5 μg recombinant IL-7 together with 7.5 μg anti-IL-7 (M25, a generous gift of C. D. Surh) were pre-incubated for 10 min at 25°C, then PBS was added up to 0.4 ml. Mice were injected *i.p*. one or two times at 3-day intervals with complexes of IL-7-M25 or PBS.

Nitric oxide measurement

Nitrite concentration was assessed using the Griess reaction

Antibodies

The following antibodies were used in this study for flow cytometry: CD8α (53-6.7), CD4 (L3T4), CD3ε (145-2C11), CD5 (J3-7.3), CD25 (PC61.5), CD45.1(A20), CD45.2 (104), CD69 (H1.2F3), IFN-γ (XMG1.2), Bcl2 (10C4), CD44 (IM7), CD122 (TM-b1), Qa-2 (1-1-2), Fas (15A7), CD11b (M1/70), TCRβ (H57-597), B220 (RA3-6B2), NK1.1 (PK 136) (eBioscience); Ly6G (1A8) (Biolegend) JNK, P-JNK, p38-MAPK, P-p38-MAPK, AKT, P-AKT (S473), P-AKT (T308) (Cell Signaling Technology); Anti-BrdU, Ly6C (AL-21), (BD Biosciences). The following antibodies were used for immunoblotting: P-p38-MAPK, p38-MAPK, ERK1/2, p65 (Cell Signaling Technology), NFAT1 (Affinity Bioreagents). Purified CD3ε (145–2C11) and CD28 (37.51) antibodies (eBioscience) were used at indicated concentrations for T cell activation. AnnexinV (BD Biosciences) was used to identify proapoptotic T cells.

Statistical analyses

The statistical significance of differences was determined by the two-tailed Student's *t*-test. Differences with a *P* value of less than 0.05 were considered statistically significant. All error bars represent SD.

Supplementary Material

Refer to Web version on PubMed Central for supplementary material.

Acknowledgements

MB and PK were each supported by EMBO long-term fellowships. PK was also supported by the Swiss National Science Foundation. This work was supported by NIH Contract no. PO1 AI070167-01. We are grateful for the helpful discussions of O. Milstein, J.F. Purton, and K. Brandl.

References

1. Yusuf I, Fruman DA. Regulation of quiescence in lymphocytes. Trends Immunol. 2003; 24:380–386. [PubMed: 12860529]
2. Chechlinska M, et al. Molecular signature of cell cycle exit induced in human T lymphoblasts by IL-2 withdrawal. BMC Genomics. 2009; 10:261. [PubMed: 19505301]

3. Coller HA, Sang L, Roberts JM. A new description of cellular quiescence. PLoS Biol. 2006; 4:e83. [PubMed: 16509772]
4. Glynne R, Ghandour G, Rayner J, Mack DH, Goodnow CC. B-lymphocyte quiescence, tolerance and activation as viewed by global gene expression profiling on microarrays. Immunol. Rev. 2000; 176:216–246. [PubMed: 11043780]
5. Teague TK, et al. Activation changes the spectrum but not the diversity of genes expressed by T cells. Proc. Natl. Acad. Sci. USA. 1999; 96:12691–12696. [PubMed: 10535984]
6. Tothova Z, et al. FoxOs are critical mediators of hematopoietic stem cell resistance to physiologic oxidative stress. Cell. 2007; 128:325–339. [PubMed: 17254970]
7. Kuo CT, Veselits ML, Leiden JM. LKLF: A transcriptional regulator of single-positive T cell quiescence and survival. Science. 1997; 277:1986–1990. [PubMed: 9302292]
8. Tzachanis D, et al. Tob is a negative regulator of activation that is expressed in anergic and quiescent T cells. Nat. Immunol. 2001; 2:1174–1182. [PubMed: 11694881]
9. Crozat K, et al. Analysis of the MCMV resistome by ENU mutagenesis. Mamm. Genome. 2006; 17:398–406. [PubMed: 16688530]
10. Webb JR, Lee SH, Vidal SM. Genetic control of innate immune responses against cytomegalovirus: MCMV meets its match 3. Genes Immun. 2002; 3:250–262. [PubMed: 12140743]
11. Jiang Z, et al. Details of Toll-like receptor:adapter interaction revealed by germ-line mutagenesis. Proc. Natl. Acad. Sci. USA. 2006; 103:10961–10966. [PubMed: 16832055]
12. Macian F. NFAT proteins: key regulators of T-cell development and function. Nat. Rev. Immunol. 2005; 5:472–484. [PubMed: 15928679]
13. Li Q, Verma IM. NF-kappaB regulation in the immune system. Nat. Rev. Immunol. 2002; 2:725–734. [PubMed: 12360211]
14. Juntilla MM, Koretzky GA. Critical roles of the PI3K/Akt signaling pathway in T cell development. Immunol. Lett. 2008; 116:104–110. [PubMed: 18243340]
15. Wada T, Penninger JM. Mitogen-activated protein kinases in apoptosis regulation. Oncogene. 2004; 23:2838–2849. [PubMed: 15077147]
16. Rincon M, Pedraza-Alva G. JNK and p38 MAP kinases in CD4+ and CD8+ T cells. Immunol. Rev. 2003; 192:131–142. [PubMed: 12670401]
17. Boyman O, Ramsey C, Kim DM, Sprent J, Surh CD. IL-7/anti-IL-7 mAb complexes restore T cell development and induce homeostatic T Cell expansion without lymphopenia. J. Immunol. 2008; 180:7265–7275. [PubMed: 18490726]
18. Kieper WC, Jameson SC. Homeostatic expansion and phenotypic conversion of naive T cells in response to self peptide/MHC ligands. Proc. Natl. Acad. Sci. USA. 1999; 96:13306–13311. [PubMed: 10557316]
19. Goldrath AW, Bogatzki LY, Bevan MJ. Naive T cells transiently acquire a memory-like phenotype during homeostasis-driven proliferation. J. Exp. Med. 2000; 192:557–564. [PubMed: 10952725]
20. Cho BK, Rao VP, Ge Q, Eisen HN, Chen J. Homeostasis-stimulated proliferation drives naive T cells to differentiate directly into memory T cells. J. Exp. Med. 2000; 192:549–556. [PubMed: 10952724]
21. Khaled AR, Durum SK. Lymphocide: cytokines and the control of lymphoid homeostasis. Nat. Rev. Immunol. 2002; 2:817–830. [PubMed: 12415306]
22. Hildeman DA, et al. Activated T cell death in vivo mediated by proapoptotic bcl-2 family member bim. Immunity. 2002; 16:759–767. [PubMed: 12121658]
23. Pellegrini M, Belz G, Bouillet P, Strasser A. Shutdown of an acute T cell immune response to viral infection is mediated by the proapoptotic Bcl-2 homology 3-only protein Bim. Proc. Natl. Acad. Sci. USA. 2003; 100:14175–14180. [PubMed: 14623954]
24. Krammer PH, Arnold R, Lavrik IN. Life and death in peripheral T cells. Nat. Rev. Immunol. 2007; 7:532–542. [PubMed: 17589543]
25. Boyman O, Cho JH, Tan JT, Surh CD, Sprent J. A major histocompatibility complex class I-dependent subset of memory phenotype CD8+ cells. J. Exp. Med. 2006; 203:1817–1825. [PubMed: 16818671]

26. Oehen S, Brduscha-Riem K. Differentiation of naive CTL to effector and memory CTL: correlation of effector function with phenotype and cell division. J. Immunol. 1998; 161:5338–5346. [PubMed: 9820507]
27. Chao CC, Jensen R, Dailey MO. Mechanisms of L-selectin regulation by activated T cells. J. Immunol. 1997; 159:1686–1694. [PubMed: 9257829]
28. Serbina NV, et al. Sequential MyD88-independent and -dependent activation of innate immune responses to intracellular bacterial infection. Immunity. 2003; 19:891–901. [PubMed: 14670305]
29. Schwarz DA, Katayama CD, Hedrick SM. Schlafen, a new family of growth regulatory genes that affect thymocyte development. Immunity. 1998; 9:657–668. [PubMed: 9846487]
30. Dooms H, et al. Quiescence-inducing and antiapoptotic activities of IL-15 enhance secondary CD4+ T cell responsiveness to antigen. J. Immunol. 1998; 161:2141–2150. [PubMed: 9725205]
31. Buckley AF, Kuo CT, Leiden JM. Transcription factor LKLF is sufficient to program T cell quiescence via a c-Myc--dependent pathway. Nat. Immunol. 2001; 2:698–704. [PubMed: 11477405]
32. Bai A, Hu H, Yeung M, Chen J. Kruppel-like factor 2 controls T cell trafficking by activating L-selectin (CD62L) and sphingosine-1-phosphate receptor 1 transcription. J. Immunol. 2007; 178:7632–7639. [PubMed: 17548599]
33. Carlson CM, et al. Kruppel-like factor 2 regulates thymocyte and T-cell migration. Nature. 2006; 442:299–302. [PubMed: 16855590]
34. Kerdiles YM, et al. Foxo1 links homing and survival of naive T cells by regulating L-selectin, CCR7 and interleukin 7 receptor. Nat. Immunol. 2009; 10:176–184. [PubMed: 19136962]
35. Geserick P, Kaiser F, Klemm U, Kaufmann SH, Zerrahn J. Modulation of T cell development and activation by novel members of the Schlafen (slfn) gene family harbouring an RNA helicase-like motif. Int. Immunol. 2004; 16:1535–1548. [PubMed: 15351786]
36. Ferguson DA, Chiang JT, Richardson JA, Graff J. eXPRESSION: an in silico tool to predict patterns of gene expression. Gene Expr. Patterns. 2005; 5:619–628. [PubMed: 15939374]
37. Hanson PI, Whiteheart SW. AAA+ proteins: have engine, will work. Nat. Rev. Mol. Cell Biol. 2005; 6:519–529. [PubMed: 16072036]
38. White SR, Lauring B. AAA+ ATPases: achieving diversity of function with conserved machinery. Traffic. 2007; 8:1657–1667. [PubMed: 17897320]
39. Brady G, Boggan L, Bowie A, O'Neill LA. Schlafen-1 causes a cell cycle arrest by inhibiting induction of cyclin D1. J. Biol. Chem. 2005; 280:30723–30734. [PubMed: 15946944]
40. Kaufmann A, et al. Defense against influenza A virus infection: essential role of the chemokine system. Immunobiology. 2001; 204:603–613. [PubMed: 11846225]
41. Barbalat R, Lau L, Locksley RM, Barton GM. Toll-like receptor 2 on inflammatory monocytes induces type I interferon in response to viral but not bacterial ligands. Nat. Immunol. 2009; 10:1200–1207. [PubMed: 19801985]
42. Gubser C, et al. Camelpox virus encodes a schlafen-like protein that affects orthopoxvirus virulence. J. Gen. Virol. 2007; 88:1667–1676. [PubMed: 17485525]
43. Hoebe K, Du X, Goode J, Mann N, Beutler B. *Lps2*: a new locus required for responses to lipopolysaccharide, revealed by germline mutagenesis and phenotypic screening. J. Endotoxin Res. 2003; 9:250–255. [PubMed: 12935356]
44. Rutschmann S, et al. PanR1, a dominant negative missense allele of the gene encoding TNF-alpha (Tnf), does not impair lymphoid development. J. Immunol. 2006; 176:7525–7532. [PubMed: 16751399]
45. Krebs P, et al. NK-cell-mediated killing of target cells triggers robust antigen-specific T-cell-mediated and humoral responses. Blood. 2009; 113:6593–6602. [PubMed: 19406986]
46. Reeves JP, Reeves PA. Removal of lymphoid organs. Curr. Protoc. Immunol. 2001 Chapter 1, Unit 1.9.

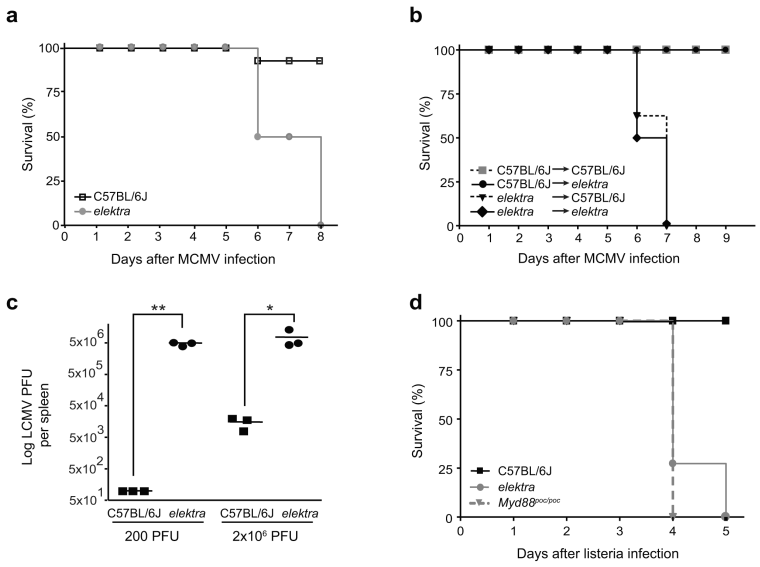

Figure 1. Homozygous *elektra* mutants are highly susceptible to MCMV, LCMV and *L. monocytogenes* infections

(a) Survival curves for WT (*n*=8) and homozygous *elektra* mutants (*n*=8) upon challenge with 2×10^5 PFU of MCMV. Results are representative of five independent experiments. **(b)** Survival curves upon infection with 2×10^5 PFU of MCMV after reciprocal bone marrow transplantation. Recipient mice were reconstituted with 5×10^6 bone marrow cells 1 day after 10-Gy dose of irradiation. Congenic C57BL/6.SJL (*Ptprc*^{a}*Pep3*^{b}*; Ly5.1*$^+$), C57BL/6J (*Ptprc*^{b}*Pep3*^{a}*; Ly5.2*$^+$) WT or *elektra* mutant mice were used as both recipients and donors as indicated in the figure. C57BL/6J into C57BL/6J, *n*=3; C57BL/6J into *elektra*, *n*=6; *elektra* into C57BL/6J, *n*=6; *elektra* into *elektra*, *n*=3. Results are representative of 2 independent experiments. **(c)** WT and homozygous *elektra* mice (3 mice in each group) were i.v. injected with either 200 or 2×10^6 PFU of LCMV (Armstrong strain). Viral load was measured in spleens 7 days after injection. Results are representative of two independent experiments. ** $P < 0.0001$, *$P = 0.028$. **(d)** Survival curves for WT (*n*=5), homozygous *elektra* (*n*=7), and *Myd88*$^{poc/poc}$ (*n*=2) mice when challenged with 2×10^5 CFU of *Listeria monocytogenes*. Results are representative of four independent experiments.

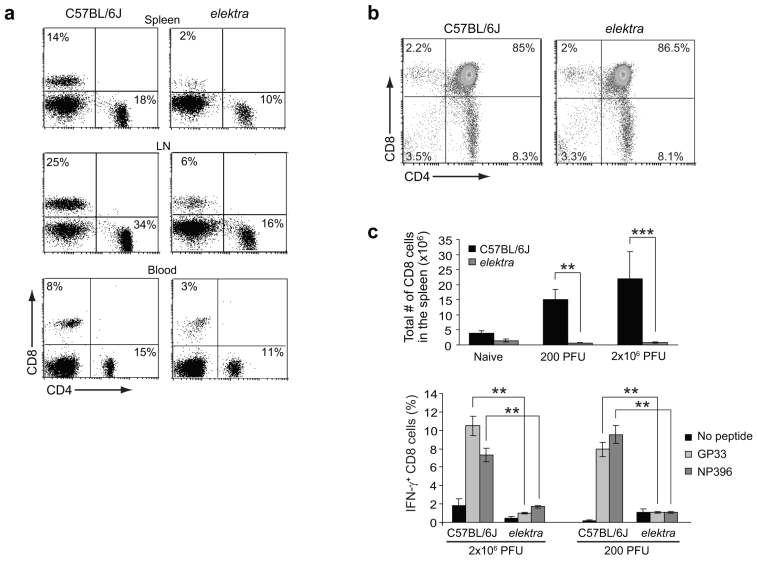

Figure 2. Defect in peripheral T cells in *elektra* homozygotes

(a) Cells from spleen, lymph node (LN), and blood of WT or homozygous *elektra* mice were analyzed by flow cytometry for CD4 and CD8 expression. **(b)** Thymocytes from WT or homozygous *elektra* mice were analyzed by flow cytometry for CD4 and CD8 expression. For **a** and **b**, results are representative of 10 mice per genotype. **(c)** WT and homozygous *elektra* mice were i.v. injected with either 200 or 2×10^6 PFU of LCMV (Armstrong strain). Splenocytes were isolated 7 days post-injection and restimulated *ex vivo* with either GP33 or NP396, peptides derived from LCMV, in the presence of Brefeldin A. Total numbers of $CD8^+$ splenocytes were determined by flow cytometry (top). $CD8^+$ cells were then fixed, permeabilized, and stained for intracellular IFN-γ expression (bottom). *n*=3 mice of each genotype per condition. Results are representative of 2 independent experiments. *** $P < 0.001$, ** $P < 0.01$.

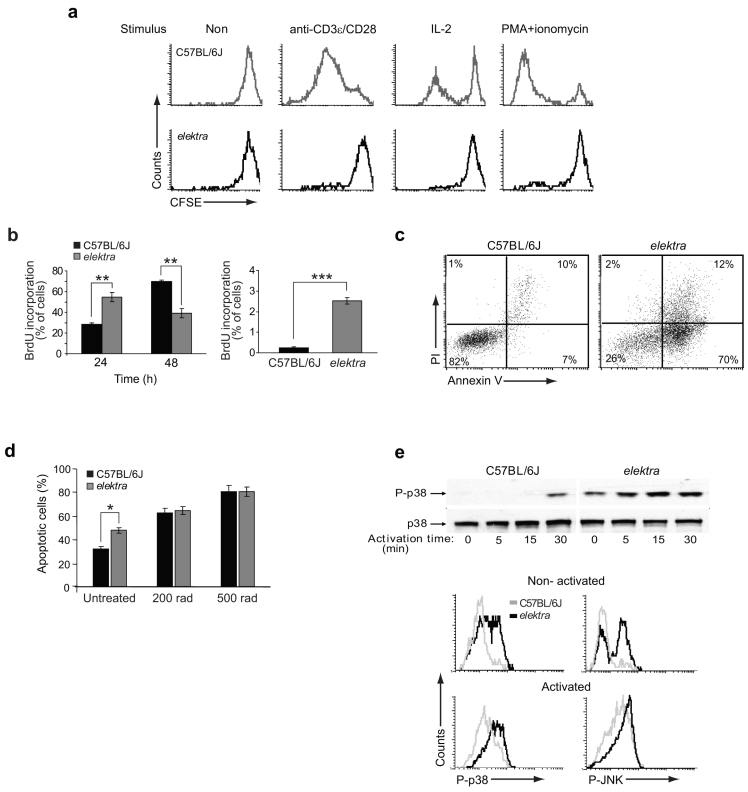

Figure 3. Apoptosis of homozygous *elektra* T cells in response to activation signals

(a) CFSE intensity of $CD8^+$ lymph node cells that were treated as indicated. Results are representative of 3 mice per genotype. **(b)** Left, BrdU incorporation measured by flow cytometry of $CD8^+$ T cells from WT or *elektra* mice (*n*=3 each) that were either untreated, or stimulated with anti-CD3ε and anti-CD28. Results are representative of two experiments. Right, BrdU incorporation measured by flow cytometry of $CD8^+$ T cells from WT or *elektra* mice (*n*=4 each) 4 h after injection with BrdU. Results are representative of two experiments. **(c)** Propidium iodide versus Annexin V staining of $CD8^+$ T cells from WT or *elektra* mice (*n*=3 each) stimulated *ex vivo* with anti-CD3ε and anti-CD28 for 48 h. Results are representative of two experiments. **(d)** Percentage of Annexin V^+ cells (gated on $CD8^+$ propidium iodide negative population) induced by γ-irradiation (*n*=3 mice each). **(e)** Immunoblot analysis (top) and flow cytometric analysis (bottom) using anti-phospho-p38-MAPK or anti-p38-MAPK of pooled $CD8^+$ T cells from WT (*n*=2) or *elektra* (*n*=4) mice upon anti-CD3ε and anti-CD28 treatment. Results are representative of 3 mice per genotype. For all panels, *** $P < 0.001$, ** $P < 0.01$, * $P < 0.05$.

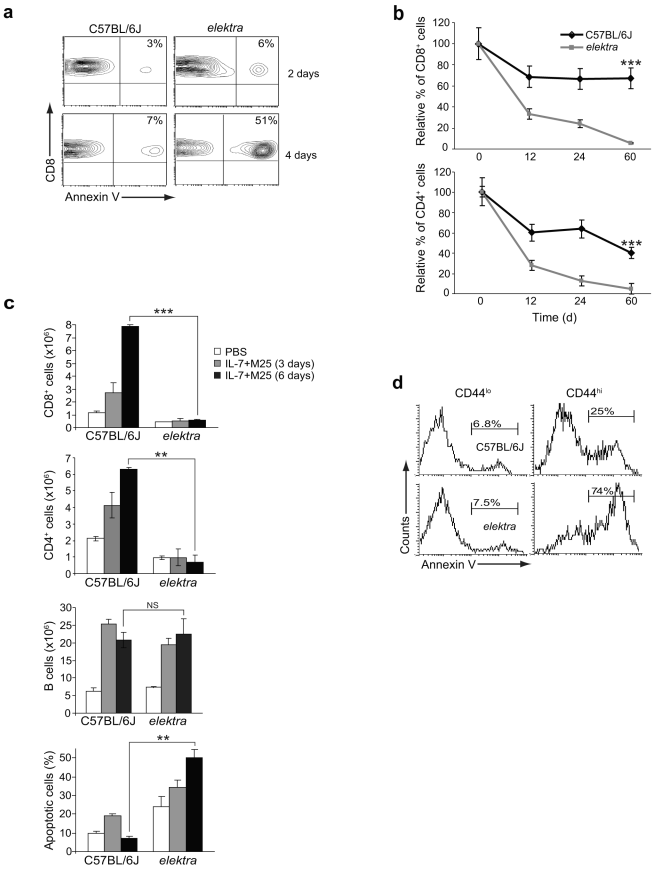

Figure 4. Apoptosis of homozygous *elektra* T cells in response to homeostatic expansion signals

(a) Annexin V staining of adoptively transferred WT or *elektra* $CD8^+CD45.1^-$ cells from spleens of WT ($Ly5.1^+$) recipient mice (n=4). Results are representative of three experiments. **(b)** Relative % of $CD8^+$ (top) or $CD4^+$ (bottom) T cells in seven week-old WT or *elektra* mice (n=5 or 6 respectively) at different time points after thymectomy. Relative % of T cells = (% T cells after thymectomy)/ (% T cells before the thymectomy). Results are representative of two experiments. **(c)** Numbers of $CD8^+$, $CD4^+$, B cells, and percentage of Annexin V positive $CD8^+$ T cells in spleens from *elektra* or WT mice (n=4 each) injected with either PBS, or IL-7/anti-IL-7 (M25). White and black bars, mice injected with either PBS or IL-7/anti-IL-7 respectively on days 1 and 3 and cells collected on day 6; gray bars, mice injected with IL-7/anti-IL-7 on day 1 and cells collected on day 3. Results are representative of two experiments. **(d)** Annexin V staining of splenic $CD8^+CD44^{hi}$ or $CD8^+CD44^{lo}$ cells from WT or *elektra* mice (n=4 each). Results are representative of 3 experiments. For all panels, *** $P < 0.001$, ** $P < 0.01$, * $P < 0.05$.

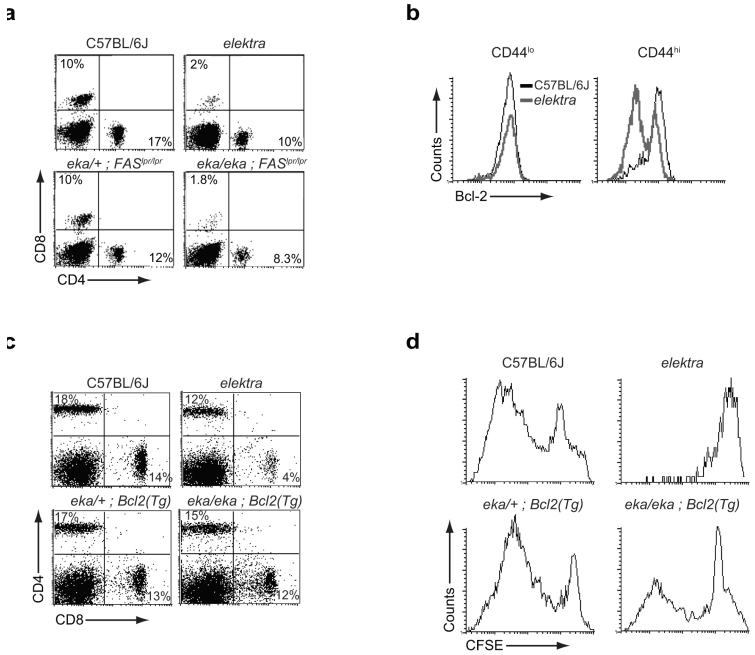

Figure 5. Homozygous *elektra* T cells die via the intrinsic apoptotic pathway

(a) *Elektra* mutant mice were crossed to *Fas*$^{lpr/lpr}$ mutant mice to generate double mutant *elektra* (*eka/eka*); *Fas*$^{lpr/lpr}$ mice. Shown, CD4 versus CD8 staining of blood cells from 6 week-old littermate mice. **(b)** Bcl-2 expression in splenic CD8^{+}CD44^{hi} or CD8^{+}CD44^{lo} cells from WT or homozygous *elektra* mice analyzed by flow cytometry. **(c)** *Elektra* mutant mice were crossed to *Tg(BCL2)25Wehi/J* transgenic mice to generate homozygous *elektra* mice overexpressing Bcl2 in T cells. CD4 versus CD8 staining of splenic cells from 4 week-old littermate mice. **(d)** CFSE-labeled spleen cells from mice used in **c** were stimulated *in vitro* with a combination of anti-CD3ε and anti-CD28. Cells were collected after 72 h and CFSE intensity of the CD3^{+} CD8^{+} cells was analyzed by flow cytometry. For all panels, results are representative of 2 independent experiments each using 3–4 mice per genotype.

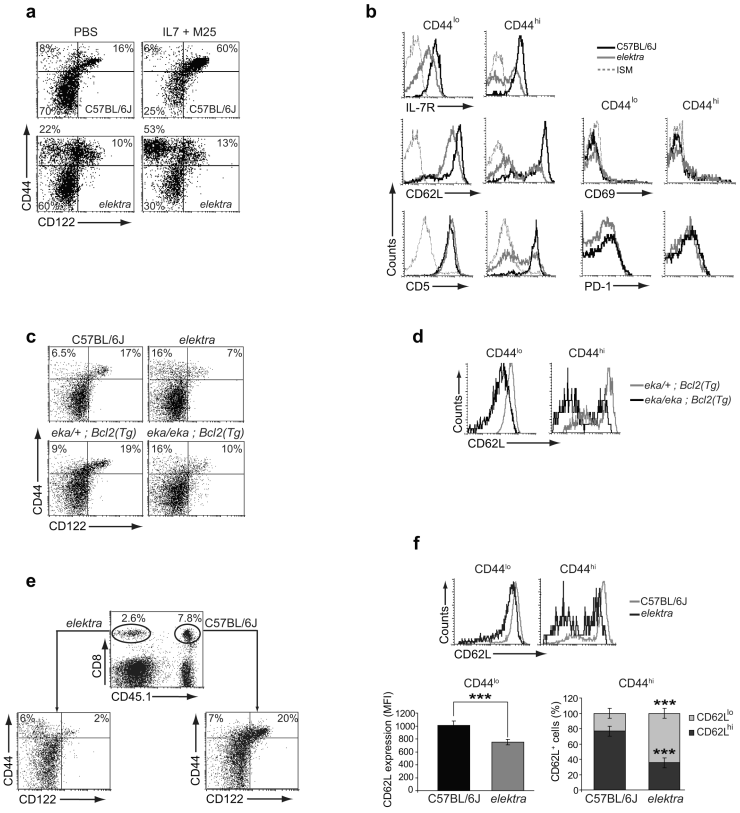

Figure 6. Homozygous *elektra* T cells exist in a semi-activated state

(a) Flow cytometric analysis of CD44 versus CD122 (IL-2Rβ) staining of splenic $CD8^+$ cells from WT or *elektra* mice injected twice (one dose every 3 days) with either PBS or IL-7/anti-IL-7 (*n*=3 per genotype). Results are representative of two experiments. **(b)** Flow cytometric analysis of IL-7Rα, CD62L, CD5, CD69, and PD-1 staining of $CD44^{lo}CD8^+$ or $CD44^{hi}CD8^+$ cells. ISM, isotype-matched control antibody (*n*=3 per genotype). Results are representative 3 experiments. **(c)** CD44 versus CD122 staining of splenic $CD8^+$ cells from 4 week-old elektra/+;Bcl2(Tg), elektra/elektra;Bcl2(Tg), elektra or WT littermate mice (*n*=3 each). **(d)** CD62L staining of spleen $CD44^{lo}CD8^+$ or $CD44^{hi}CD8^+$ cells from *elektra/+;Bcl2(Tg)* and *elektra/elektra;Bcl2(Tg)* mice (*n*=3 each). For **c** and **d** results are representative of two experiments. **(e,f)** Flow cytometric analysis of WT ($CD45.1^+$) and *elektra* ($CD45.2^+$) donor $CD8^+$ T cells in CD3-deficient mixed bone marrow chimeras. **(e)** CD44 versus CD122 staining. **(f)** CD62L staining of $CD44^{lo}CD8^+$ or $CD44^{hi}CD8^+$ cells. Top, representative flow cytometry plots. Bottom, averaged mean fluorescence intensity (MFI) of CD62L staining in the $CD44^{lo}$ population; and percentages of $CD62L^{hi}$ and $CD62L^{lo}$ expressing cells in the $CD44^{hi}$ population. For **e** and **f,** *n*=6 recipient mice, *** $P < 0.001$.

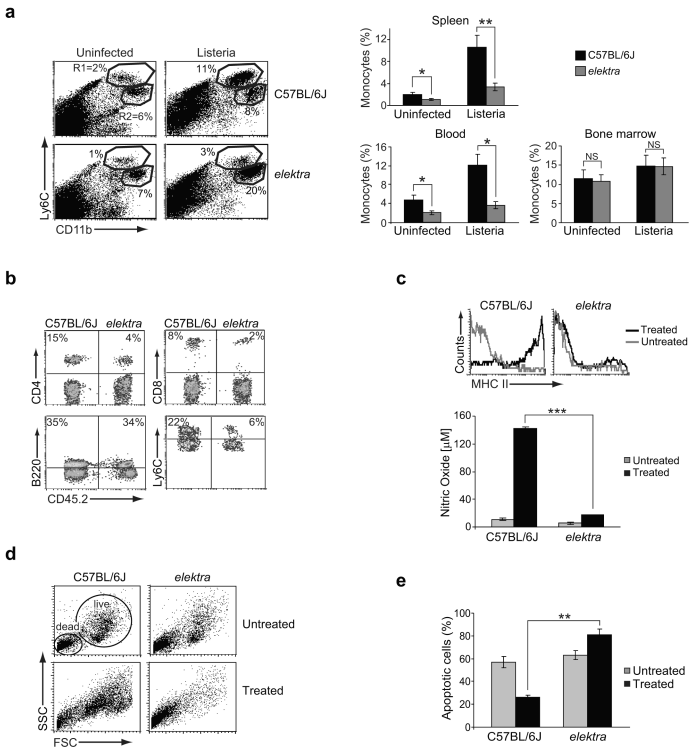

Figure 7. Apoptosis of homozygous *elektra* monocytes in response to activation signals

(a) Left, Ly6C versus CD11b staining of splenocytes from uninfected or *L. monocytogenes* infected WT or *elektra* mice (*n*=5 per genotype). Percentages of inflammatory monocytes and neutrophils are indicated by R1 and R2 gated cell populations, respectively. Results are representative of 3 experiments. Right, average percentage of inflammatory monocytes 48 h post-infection from spleen, blood, and bone marrow of WT or *elektra* mice (*n*=5 each). **(b)** Flow cytometric analysis of WT ($CD45.1^+$) and *elektra* ($CD45.2^+$) donor $CD4^+$, $CD8^+$, B cells ($B220^+$), and inflammatory monocytes (gated on $CD11b^+$ population) in the blood of CD3-deficient mixed bone marrow chimeras (*n*=3). Results are representative of two experiments. **(c–e)** Isolated bone marrow inflammatory monocytes from WT or *elektra* mice (*n*=2 each) cultured for 3 days in medium (untreated) or in medium supplemented with IFN-γ and heat-killed *L. monocytogenes* (treated). **(c)** Top, MHC class II staining. Bottom, nitric oxide concentration. **(d)** Forward-scatter (FSC) versus side-scatter (SSC) profile. Populations of live and dead cells are indicated. **(e)** Annexin V staining of the gated high FSC population. Results are representative of three experiments. For all panels, *** $P < 0.001$, ** $P < 0.01$, * $P < 0.05$. NS, not significant.

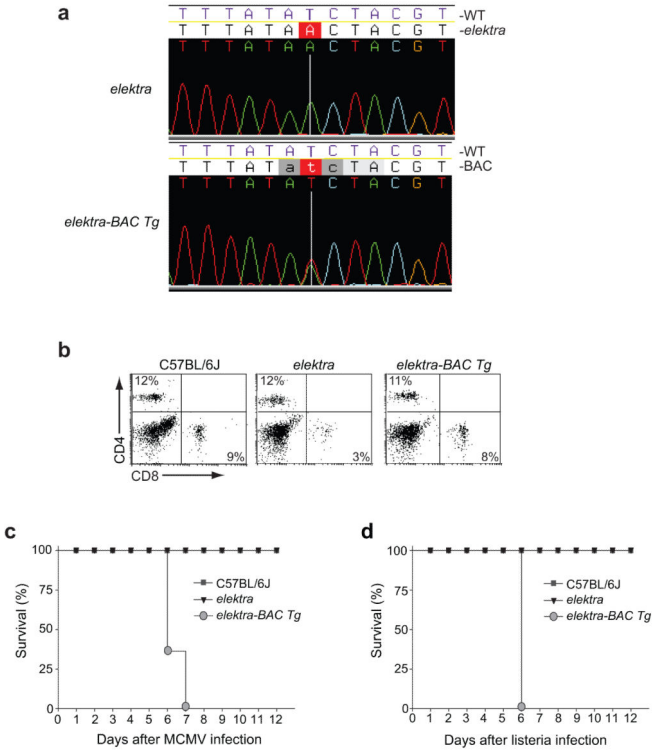

Figure 8. Rescue of the *elektra* phenotype by BAC transgenesis

Transgenic mice were produced by microinjecting a BAC clone containing the wild-type *Slfn2* sequence into single-cell embryos homozygous for the *elektra* mutation. **(a)** DNA sequence of the BAC clone and genomic DNA from an *elektra* homozygote in the region of the $Slfn2^{elektra}$ mutation. The BAC clone contains the wild-type *Slfn2* sequence. **(b)** Flow cytometric analysis of CD8 and CD4 staining of blood from a WT mouse, a homozygous *elektra* transgenic mouse carrying the *Slfn2* transgene (*elektra-BAC Tg*), and a littermate lacking the transgene (*elektra*). Results are representative of 4 mice per genotype. **(c)** Survival curves for transgenic mice (*elektra-BAC Tg*, *n*=7), littermates without the transgene (*elektra*, *n*=4), and WT mice (*n*=5) upon challenge with 2×10^5 PFU of MCMV. **(d)** Survival curves for transgenic mice (*elektra-BAC Tg*, *n*=7), littermates without the transgene (*elektra*, *n*=5), and WT mice (*n*=7) upon challenge with 5×10^5 CFU of *L. monocytogenes*.